# The $(g-2)_\mu$ in the Standard Model: review of the calculation of hadronic contributions

Gilberto Colangelo

UNIVERSITÄT BERN

AEC
ALBERT EINSTEIN CENTER
FOR FUNDAMENTAL PHYSICS

Laboratori Nazionali del Gran Sasso
9 Settembre 2021

# Outline

# Outline

Introduction: $(g-2)_\mu$ in the Standard Model
- Present status

Hadronic Vacuum Polarization contribution to $(g-2)_\mu$

Hadronic light-by-light contribution to $(g-2)_\mu$
- Dispersive approach to the hadronic light-by-light tensor
- A dispersion relation for HLbL
- Short-distance constraints

Conclusions and Outlook

# History of $a_\mu$ measurements

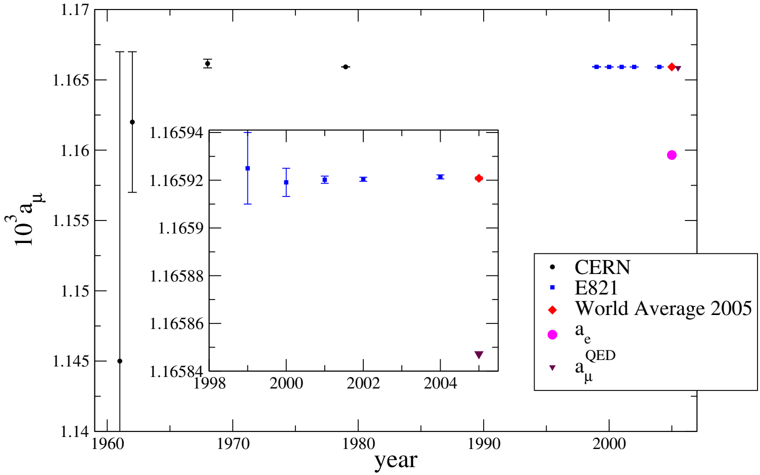

# $a_\mu$, QED and the SM

World Average (before FNAL)

$$a_\mu^{\rm exp} = (116\,592\,089 \pm 63) \times 10^{-11}$$

# $a_\mu$, QED and the SM

World Average (before FNAL)

$$a_\mu^{\mathrm{exp}} = (116\,592\,089 \pm 63) \times 10^{-11}$$

- The bulk of the difference between $a_e$ and $a_\mu$ is due to QED and originates from large logs of $m_\mu/m_e$

$$a_\mu^{\mathrm{QED}} - a_e^{\mathrm{QED}} = 619\,500.2 \times 10^{-11}$$

# $a_\mu$, QED and the SM

World Average (before FNAL)

$$a_\mu^{\text{exp}} = (116\,592\,089 \pm 63) \times 10^{-11}$$

- The bulk of the difference between $a_e$ and $a_\mu$ is due to QED and originates from large logs of $m_\mu/m_e$

$$a_\mu^{\text{QED}} - a_e^{\text{QED}} = 619\,500.2 \times 10^{-11}$$
$$a_\mu^{\text{exp}} - a_\mu^{\text{QED}} = (7360 \pm 63) \times 10^{-11}$$

# $a_\mu$, QED and the SM

World Average (before FNAL)

$$a_\mu^{\text{exp}} = (116\,592\,089 \pm 63) \times 10^{-11}$$

- The bulk of the difference between $a_e$ and $a_\mu$ is due to QED and originates from large logs of $m_\mu/m_e$

$$a_\mu^{\text{QED}} - a_e^{\text{QED}} = 619\,500.2 \times 10^{-11}$$
$$a_\mu^{\text{exp}} - a_\mu^{\text{QED}} = (7360 \pm 63) \times 10^{-11}$$

- Hadronic contributions are large

$$a_\mu^{\text{had}} \simeq 7000 \times 10^{-11}$$

"Seen" at the $5\sigma$ level already in 1979

# $a_\mu$, QED and the SM

World Average (before FNAL)

$$a_\mu^{\mathrm{exp}} = (116\,592\,089 \pm 63) \times 10^{-11}$$

- The bulk of the difference between $a_e$ and $a_\mu$ is due to QED and originates from large logs of $m_\mu/m_e$

$$a_\mu^{\mathrm{QED}} - a_e^{\mathrm{QED}} = 619\,500.2 \times 10^{-11}$$
$$a_\mu^{\mathrm{exp}} - a_\mu^{\mathrm{QED}} = (7360 \pm 63) \times 10^{-11}$$

- Hadronic contributions are large

$$a_\mu^{\mathrm{had}} \simeq 7000 \times 10^{-11}$$

  "Seen" at the $5\sigma$ level already in 1979
- Weak contributions to $a_\mu$

$$a_\mu^{\mathrm{EW}} = 154 \times 10^{-11} \simeq 2.5 \Delta a_\mu^{\mathrm{exp}}$$

# Present status of $(g-2)_\mu$, experiment vs SM

$$a_\mu(BNL) = 116\,592\,089(63) \times 10^{-11}$$

$$a_\mu(FNAL) = 116\,592\,040(54) \times 10^{-11}$$

$$a_\mu(Exp) = 116\,592\,061(41) \times 10^{-11}$$

# Present status of $(g-2)_\mu$, experiment vs SM

Before the Fermilab result

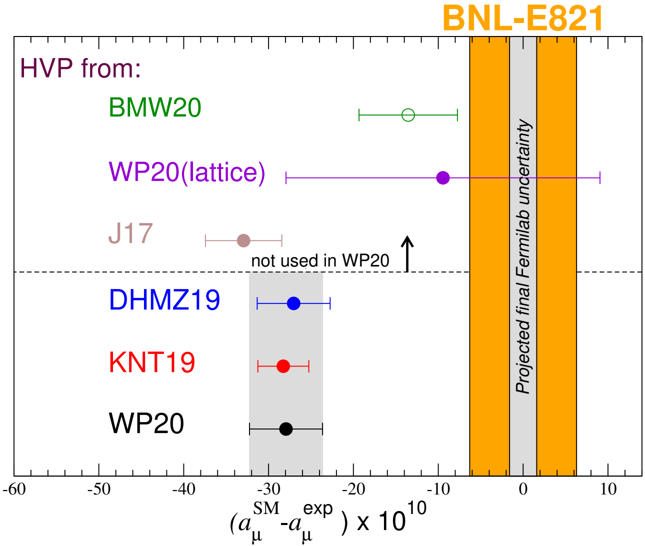

# Present status of $(g-2)_\mu$, experiment vs SM

After the Fermilab result

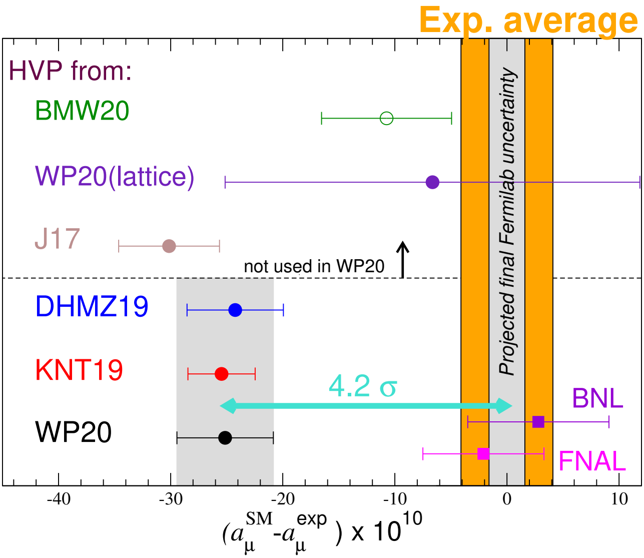

# White Paper (2020): $(g-2)_\mu$, experiment vs SM

| Contribution | Value $\times 10^{11}$ |
|---|---|
| HVP LO ($e^+e^-$) | 6931(40) |
| HVP NLO ($e^+e^-$) | $-98.3(7)$ |
| HVP NNLO ($e^+e^-$) | 12.4(1) |
| HVP LO (lattice , *udsc*) | 7116(184) |
| HLbL (phenomenology) | 92(19) |
| HLbL NLO (phenomenology) | 2(1) |
| HLbL (lattice, *uds*) | 79(35) |
| HLbL (phenomenology + lattice) | 90(17) |
| QED | 116 584 718.931(104) |
| Electroweak | 153.6(1.0) |
| HVP ($e^+e^-$, LO + NLO + NNLO) | 6845(40) |
| HLbL (phenomenology + lattice + NLO) | 92(18) |
| Total SM Value | 116 591 810(43) |
| Experiment | 116 592 061(41) |
| Difference: $\Delta a_\mu := a_\mu^{\text{exp}} - a_\mu^{\text{SM}}$ | 251(59) |

# White Paper (2020): $(g-2)_\mu$, experiment vs SM

| Contribution | Value $\times 10^{11}$ |
|---|---|
| HVP LO ($e^+e^-$) | 6931(40) |
| HVP NLO ($e^+e^-$) | −98.3(7) |
| HVP NNLO ($e^+e^-$) | 12.4(1) |
| HVP LO (lattice BMW(20), *udsc*) | 7075(55) |
| HLbL (phenomenology) | 92(19) |
| HLbL NLO (phenomenology) | 2(1) |
| HLbL (lattice, *uds*) | 79(35) |
| HLbL (phenomenology + lattice) | 90(17) |
| QED | 116 584 718.931(104) |
| Electroweak | 153.6(1.0) |
| HVP ($e^+e^-$, LO + NLO + NNLO) | 6845(40) |
| HLbL (phenomenology + lattice + NLO) | 92(18) |
| Total SM Value | 116 591 810(43) |
| Experiment | 116 592 061(41) |
| Difference: $\Delta a_\mu := a_\mu^{\text{exp}} - a_\mu^{\text{SM}}$ | 251(59) |

# White Paper (2020): $(g-2)_\mu$, experiment vs SM

**White Paper**:
T. Aoyama et al. Phys. Rep. 887 (2020) = WP(20)

**Muon $g-2$ Theory Initiative**
Steering Committee:
GC
Michel Davier (vice-chair)
Simon Eidelman
Aida El-Khadra (chair)
Martin Hoferichter
Christoph Lehner (vice-chair)
Tsutomu Mibe (J-PARC E34 experiment)
(*Andreas Nyffeler* until summer 2020)
Lee Roberts (Fermilab E989 experiment)
Thomas Teubner
Hartmut Wittig

# White Paper (2020): $(g-2)_\mu$, experiment vs SM

**White Paper**:
T. Aoyama et al. Phys. Rep. 887 (2020) = WP(20)

**Muon $g-2$ Theory Initiative**
Workshops:

- First plenary meeting, Q-Center (Fermilab), 3-6 June 2017
- HVP WG workshop, KEK (Japan), 12-14 February 2018
- HLbL WG workshop, U. of Connecticut, 12-14 March 2018
- Second plenary meeting, Mainz, 18-22 June 2018
- Third plenary meeting, Seattle, 9-13 September 2019
- Lattice HVP workshop, virtual, 16-20 November 2020
- Fourth plenary meeting, KEK (virtual), 28 June-02 July 2021

# White Paper executive summary (my own)

- QED and EW known and stable, negligible uncertainties
- HVP dispersive: consensus number, conservative uncertainty (KNT19, DHMZ19, CHS19, HHK19)
- HVP lattice: consensus number, $\Delta a_\mu^{\rm HVP,latt} \sim 5\,\Delta a_\mu^{\rm HVP,disp}$ (Fermilab-HPQCD-MILC18,20, BMW18, RBC/UKQCD18, ETM19,SK19, Mainz19, ABTGJP20)
- HVP BMW20: central value $\to$ discrepancy $< 2\sigma$; $\Delta a_\mu^{\rm HVP,BMW} \sim \Delta a_\mu^{\rm HVP,disp}$ published 04/21 $\to$ not in WP
- HLbL dispersive: consensus number, w/ recent improvements $\Rightarrow$ $\Delta a_\mu^{\rm HLbL} \sim 0.5\,\Delta a_\mu^{\rm HVP}$
- HLbL lattice: single calculation, agrees with dispersive ($\Delta a_\mu^{\rm HLbL,latt} \sim 2\,\Delta a_\mu^{\rm HLbL,disp}$) $\to$ final average (RBC/UKQCD20)

# Theory uncertainty comes from hadronic physics

- Hadronic contributions responsible for most of the theory uncertainty
- Hadronic vacuum polarization (HVP) is $\mathcal{O}(\alpha^2)$, dominates the total uncertainty, despite being known to $< 1\%$

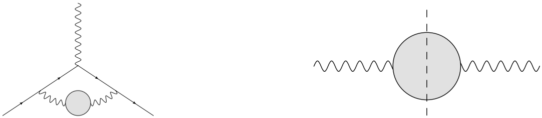

  - unitarity and analyticity $\Rightarrow$ dispersive approach
  - $\Rightarrow$ direct relation to experiment: $\sigma_{\rm tot}(e^+e^- \to \text{hadrons})$
  - $e^+e^-$ Exps: BaBar, Belle, BESIII, CMD2/3, KLOE2, SND
  - alternative approach: lattice, becoming competitive

(BMW, ETMC, Fermilab, HPQCD, Mainz, MILC, RBC/UKQCD)

# Theory uncertainty comes from hadronic physics

- Hadronic contributions responsible for most of the theory uncertainty
- Hadronic vacuum polarization (HVP) is $\mathcal{O}(\alpha^2)$, dominates the total uncertainty, despite being known to $< 1\%$
- Hadronic light-by-light (HLbL) is $\mathcal{O}(\alpha^3)$, known to $\sim 20\%$, second largest uncertainty (now subdominant)

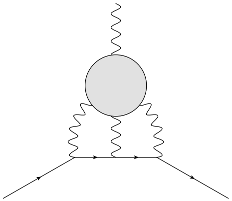

- earlier: "*it cannot be expressed in terms of measurable quantities*"
- recently: dispersive approach $\Rightarrow$ data-driven, systematic treatment
- lattice QCD is becoming competitive

(Mainz, RBC/UKQCD)

# Outline

Introduction: $(g-2)_\mu$ in the Standard Model
- Present status

Hadronic Vacuum Polarization contribution to $(g-2)_\mu$

Hadronic light-by-light contribution to $(g-2)_\mu$
- Dispersive approach to the hadronic light-by-light tensor
- A dispersion relation for HLbL
- Short-distance constraints

Conclusions and Outlook

# Hadronic vacuum polarization

$$\Pi_{\mu\nu}(q) = i\int d^4x e^{iqx}\langle 0|Tj_\mu(x)j_\nu(0)|0\rangle = \left(q_\mu q_\nu - g_{\mu\nu}q^2\right)\Pi(q^2)$$

where $j^\mu(x) = \sum_i Q_i\bar{q}_i(x)\gamma^\mu q_i(x)$, $i = u, d, s$ is the em current

- Lorentz invariance: 2 structures
- gauge invariance: reduction to 1 structure
- Lorentz-tensor defined in such a way that the function $\Pi(q^2)$ does not have kinematic singularities or zeros
- $\bar{\Pi}(q^2) := \Pi(q^2) - \Pi(0)$ satisfies

$$\bar{\Pi}(q^2) = \frac{q^2}{\pi}\int_{4M_\pi^2}^\infty dt\,\frac{\mathrm{Im}\bar{\Pi}(t)}{t(t-q^2)}$$

# Hadronic vacuum polarization

$$\Pi_{\mu\nu}(q) = i\int d^4x e^{iqx}\langle 0|Tj_\mu(x)j_\nu(0)|0\rangle = \left(q_\mu q_\nu - g_{\mu\nu}q^2\right)\Pi(q^2)$$

where $j^\mu(x) = \sum_i Q_i\bar{q}_i(x)\gamma^\mu q_i(x)$, $i = u, d, s$ is the em current

- Lorentz invariance: 2 structures
- gauge invariance: reduction to 1 structure
- Lorentz-tensor defined in such a way that the function $\Pi(q^2)$ does not have kinematic singularities or zeros
- $\bar{\Pi}(q^2) := \Pi(q^2) - \Pi(0)$ satisfies

$$\bar{\Pi}(q^2) = \frac{q^2}{\pi}\int_{4M_\pi^2}^\infty dt\frac{\mathrm{Im}\bar{\Pi}(t)}{t(t-q^2)}$$

Easy!

# HVP contribution: Master Formula

Unitarity relation: simple, same for all intermediate states

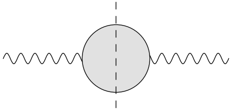

$$\mathrm{Im}\bar{\Pi}(q^2) \propto \sigma(e^+e^- \to \mathrm{hadrons}) = \sigma(e^+e^- \to \mu^+\mu^-)R(q^2)$$

Analyticity $\left[\bar{\Pi}(q^2) = \frac{q^2}{\pi}\int ds \frac{\mathrm{Im}\bar{\Pi}(s)}{s(s-q^2)}\right] \Rightarrow$ Master formula for HVP

Bouchiat, Michel (61)

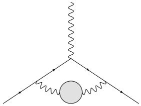

$$\Leftrightarrow \qquad a_\mu^{\mathrm{hvp}} = \frac{\alpha^2}{3\pi^2}\int_{s_{th}}^{\infty}\frac{ds}{s}K(s)R(s)$$

$K(s)$ known, depends on $m_\mu$ and $K(s) \sim \frac{1}{s}$ for large $s$

# Comparison between DHMZ19 and KNT19

| | DHMZ19 | KNT19 | Difference |
|---|---|---|---|
| $\pi^+\pi^-$ | 507.85(0.83)(3.23)(0.55) | 504.23(1.90) | 3.62 |
| $\pi^+\pi^-\pi^0$ | 46.21(0.40)(1.10)(0.86) | 46.63(94) | −0.42 |
| $\pi^+\pi^-\pi^+\pi^-$ | 13.68(0.03)(0.27)(0.14) | 13.99(19) | −0.31 |
| $\pi^+\pi^-\pi^0\pi^0$ | 18.03(0.06)(0.48)(0.26) | 18.15(74) | −0.12 |
| $K^+K^-$ | 23.08(0.20)(0.33)(0.21) | 23.00(22) | 0.08 |
| $K_S K_L$ | 12.82(0.06)(0.18)(0.15) | 13.04(19) | −0.22 |
| $\pi^0\gamma$ | 4.41(0.06)(0.04)(0.07) | 4.58(10) | −0.17 |
| Sum of the above | 626.08(0.95)(3.48)(1.47) | 623.62(2.27) | 2.46 |
| $[1.8, 3.7]$ GeV (without $c\bar{c}$) | 33.45(71) | 34.45(56) | −1.00 |
| $J/\psi$, $\psi(2S)$ | 7.76(12) | 7.84(19) | −0.08 |
| $[3.7, \infty)$ GeV | 17.15(31) | 16.95(19) | 0.20 |
| Total $a_\mu^{\text{HVP, LO}}$ | $694.0(1.0)(3.5)(1.6)(0.1)_\psi(0.7)_{\text{DV+QCD}}$ | 692.8(2.4) | 1.2 |

# $2\pi$: comparison with the dispersive approach

The $2\pi$ channel can itself be described dispersively $\Rightarrow$ more constrained theoretically Ananthanarayan, Caprini, Das (19), GC, Hoferichter, Stoffer (18)

| Energy range | ACD18 | CHS18 | DHMZ19 | KNT19 |
|---|---|---|---|---|
| $\leq 0.6\,\mathrm{GeV}$ | | 110.1(9) | 110.4(4)(5) | 108.7(9) |
| $\leq 0.7\,\mathrm{GeV}$ | | 214.8(1.7) | 214.7(0.8)(1.1) | 213.1(1.2) |
| $\leq 0.8\,\mathrm{GeV}$ | | 413.2(2.3) | 414.4(1.5)(2.3) | 412.0(1.7) |
| $\leq 0.9\,\mathrm{GeV}$ | | 479.8(2.6) | 481.9(1.8)(2.9) | 478.5(1.8) |
| $\leq 1.0\,\mathrm{GeV}$ | | 495.0(2.6) | 497.4(1.8)(3.1) | 493.8(1.9) |
| $[0.6, 0.7]\,\mathrm{GeV}$ | | 104.7(7) | 104.2(5)(5) | 104.4(5) |
| $[0.7, 0.8]\,\mathrm{GeV}$ | | 198.3(9) | 199.8(0.9)(1.2) | 198.9(7) |
| $[0.8, 0.9]\,\mathrm{GeV}$ | | 66.6(4) | 67.5(4)(6) | 66.6(3) |
| $[0.9, 1.0]\,\mathrm{GeV}$ | | 15.3(1) | 15.5(1)(2) | 15.3(1) |
| $\leq 0.63\,\mathrm{GeV}$ | 132.9(8) | 132.8(1.1) | 132.9(5)(6) | 131.2(1.0) |
| $[0.6, 0.9]\,\mathrm{GeV}$ | | 369.6(1.7) | 371.5(1.5)(2.3) | 369.8(1.3) |
| $\left[\sqrt{0.1}, \sqrt{0.95}\,\right]\,\mathrm{GeV}$ | | 490.7(2.6) | 493.1(1.8)(3.1) | 489.5(1.9) |

WP(20)

# Combination method and final result

Complete analyses DHMZ19 and KNT19, as well as CHS19 ($2\pi$) and HHK19 ($3\pi$), have been so combined:

- central values are obtained by simple averages (for each channel and mass range)
- the largest experimental and systematic uncertainty of DHMZ and KNT is taken
- $1/2$ difference DHMZ$-$KNT (or BABAR$-$KLOE in the $2\pi$ channel, if larger) is added to the uncertainty

Final result:

$$\begin{aligned} a_\mu^{\text{HVP, LO}} &= 693.1(2.8)_{\text{exp}}(2.8)_{\text{sys}}(0.7)_{\text{DV+QCD}} \times 10^{-10} \\ &= 693.1(4.0) \times 10^{-10} \end{aligned}$$

WP(20)

# The BMW result

Borsanyi et al. Nature 2021

State-of-the-art lattice calculation of $a_\mu^{\text{HVP, LO}}$ based on

- current-current correlator, summed over all distances, integrated in time with appropriate kernel function
- using staggered fermions on an $L \sim 6$ fm lattice ($L \sim 11$fm used for finite volume corrections)
- at (and around) physical quark masses
- including isospin-breaking effects

# The BMW result

Borsanyi et al. Nature 2021

## Isospin-symmetric

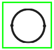
Connected light
$633.7(2.1)_{stat}(4.2)_{syst}$

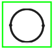
Connected strange
$53.393(89)_{stat}(68)_{syst}$

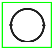
Connected charm
$14.6(0)_{stat}(1)_{syst}$

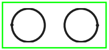
Disconnected
$-13.36(1.18)_{stat}(1.36)_{syst}$

## QED isospin breaking: valence

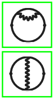
Connected $-1.23(40)_{stat}(31)_{syst}$

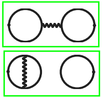
Disconnected $-0.55(15)_{stat}(10)_{syst}$

## Strong–isospin breaking

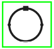
Connected
$6.60(63)_{stat}(53)_{syst}$

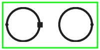
Disconnected
$-4.67(54)_{stat}(69)_{syst}$

## QED isospin breaking: sea

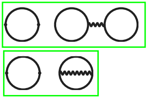
Connected $0.37(21)_{stat}(24)_{syst}$

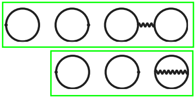
Disconnected $-0.040(33)_{stat}(21)_{syst}$

## Other

Bottom; higher-order; perturbative

$0.11(4)_{tot}$

## QED isospin breaking: mixed

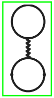
Connected $-0.0093(86)_{stat}(95)_{syst}$

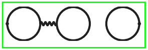
Disconnected $0.011(24)_{stat}(14)_{syst}$

## Finite-size effects

Isospin-symmetric

$18.7(2.5)_{tot}$

Isospin-breaking

$0.0(0.1)_{tot}$

$$a_\mu^{\text{LO-HVP}}\,(\times 10^{10}) = 707.5(2.3)_{stat}(5.0)_{syst}(5.5)_{tot}$$

# The BMW result

Borsanyi et al. Nature 2021

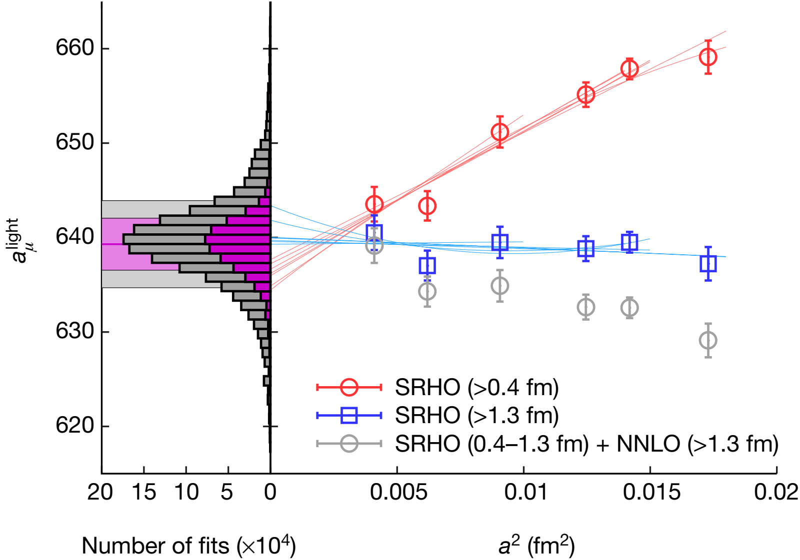

# The BMW result

Borsanyi et al. Nature 2021

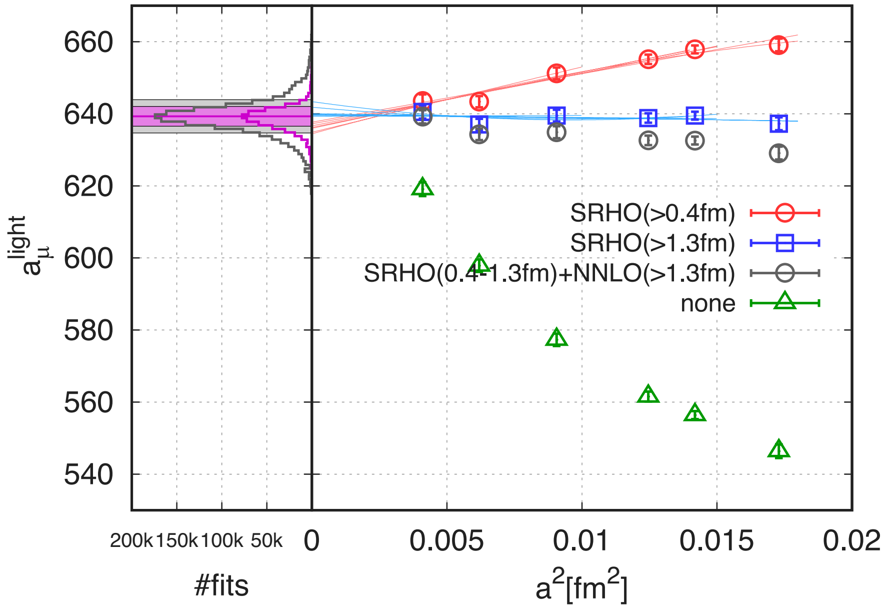

# The BMW result

Borsanyi et al. Nature 2021

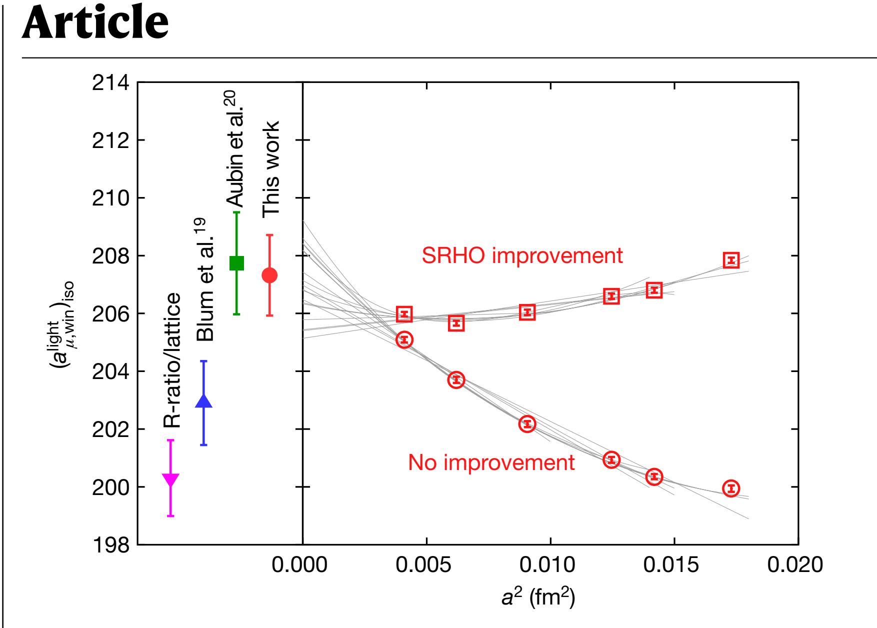

# The BMW result

Borsanyi et al. Nature 2021

## Weight functions for window quantities

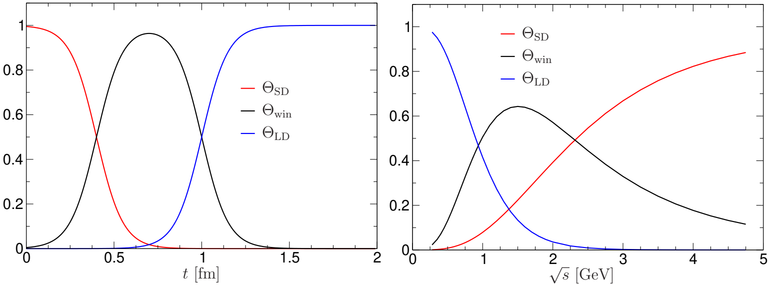

# The BMW result

Borsanyi et al. Nature 2021

## Summary: *ud* contribution

| $f$ | $a_\mu^{SD}(f)\cdot 10^{10}$ | $a_\mu^{W}(f)\cdot 10^{10}$ | $a_\mu^{LD}(f)\cdot 10^{10}$ |
|---|---|---|---|
| $ud$ | 48.2 (0.8) | 202.2 (2.6) | 382.5 (11.7) |

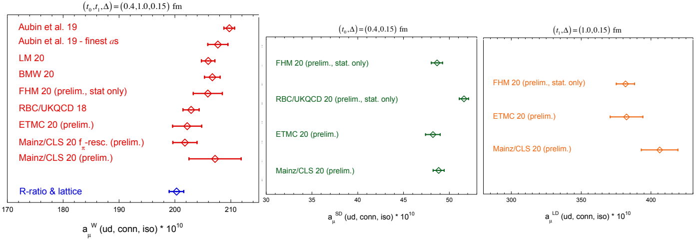


13

D. Giusti, talk at Lattice 2021

# Consequences of the BMW result

A shift in the value of $a_\mu^{\text{HVP, LO}}$ would have consequences:

- $\Delta a_\mu^{\text{HVP, LO}} \quad \Leftrightarrow \quad \Delta\sigma(e^+e^- \to \text{hadrons})$
- $\Delta\alpha_{\text{had}}(M_Z^2)$ is determined by an integral of the same $\sigma(e^+e^- \to \text{hadrons})$ (more weight at high energy)
- changing $a_\mu^{\text{HVP, LO}}$ necessarily implies a shift in $\Delta\alpha_{\text{had}}(M_Z^2)$: size depends on the energy range of $\Delta\sigma(e^+e^- \to \text{hadrons})$
- a shift in $\Delta\alpha_{\text{had}}(M_Z^2)$ has an impact on the EW-fit
- to save the EW-fit $\Delta\sigma(e^+e^- \to \text{hadrons})$ must occur below $\sim 1$ (max 2) GeV

  Crivellin, Hoferichter, Manzari, Montull (20)/Keshavarzi, Marciano, Passera, Sirlin (20)/Malaescu, Schott (20)
- or the need for BSM physics would be moved elsewhere

# Changes in $\sigma(e^+e^- \to \text{hadrons})$ below 1 GeV?

- Below $1-2$ GeV only one significant channel: $\pi^+\pi^-$
- Strongly constrained by analyticity and unitarity ($F_\pi^V(s)$)
- $F_\pi^V(s)$ parametrization which satisfies these
  $\Rightarrow$ small number of parameters GC, Hoferichter, Stoffer (18)
- $\Delta a_\mu^{\text{HVP, LO}} \quad \Leftrightarrow \quad$ shifts in these parameters
  analysis of the corresponding scenarios GC, Hoferichter, Stoffer (21)

# Changes in $\sigma(e^+e^- \to \text{hadrons})$ below 1 GeV?

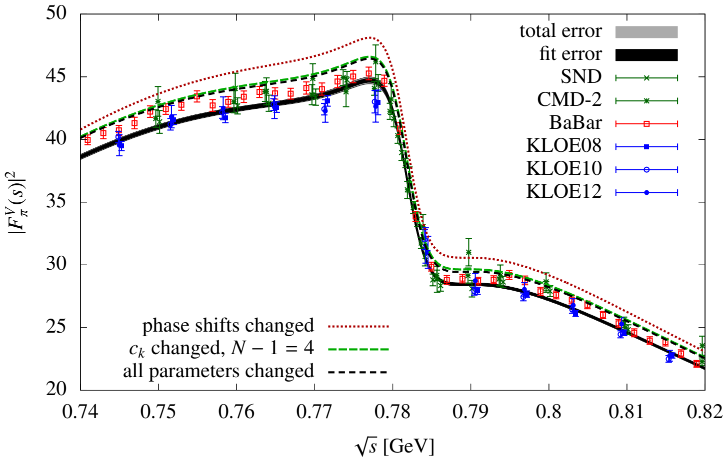


GC, Hoferichter, Stoffer (21)

Tension [BMW20 vs $e^+e^-$ data] stronger for KLOE than for BABAR

# Changes in $\sigma(e^+e^- \to \text{hadrons})$ below 1 GeV?

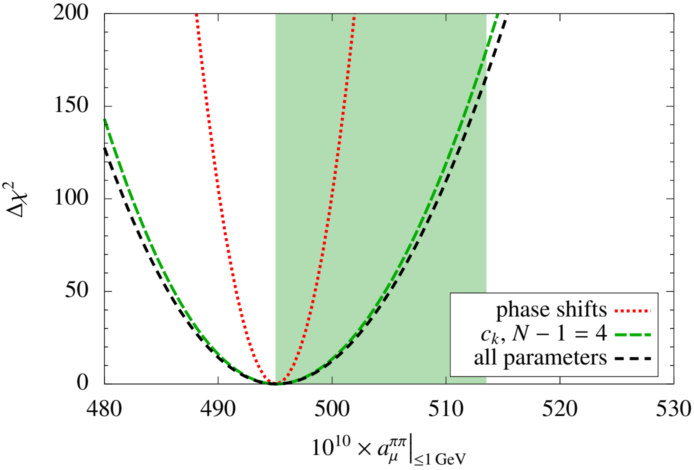


GC, Hoferichter, Stoffer (21)

# Changes in $\sigma(e^+e^- \to \text{hadrons})$ below 1 GeV?

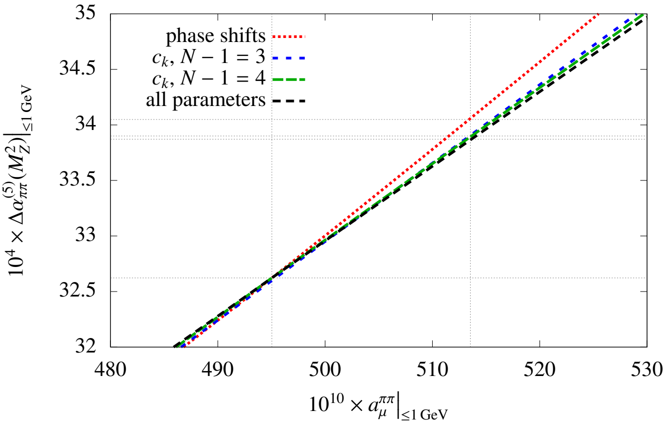


GC, Hoferichter, Stoffer (21)

$$10^4 \Delta\alpha^{(5)}_{\text{had}}(M_Z^2) = \begin{cases} 272.2(4.1) & \text{EW fit} \\ 276.1(1.1) & \sigma_{\text{had}}(s) \end{cases}$$

# Changes in $\sigma(e^+e^- \to \text{hadrons})$ below 1 GeV?

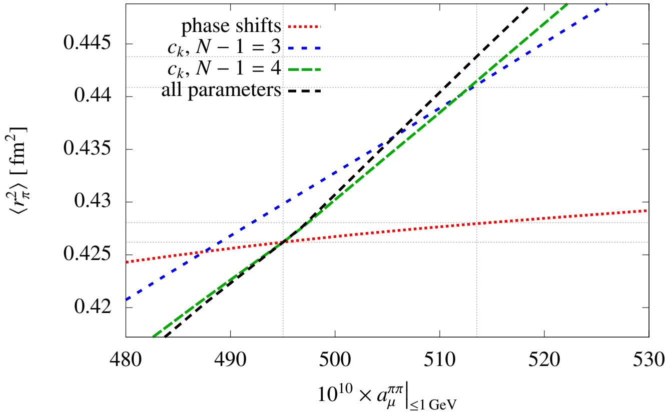


GC, Hoferichter, Stoffer (21)

$$\langle r_\pi^2 \rangle = \begin{cases} 0.429(4)\text{fm}^2 & \text{CHS(18)} \\ 0.436(5)(12)\text{fm}^2 & \chi\text{QCD(20)} \end{cases}$$

# Changes in $\sigma(e^+e^- \to \text{hadrons})$ below 1 GeV?

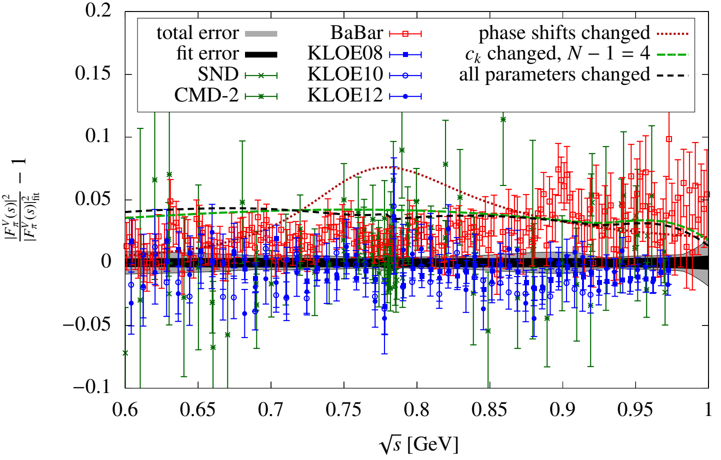


GC, Hoferichter, Stoffer (21)

# Changes in $\sigma(e^+e^- \to \text{hadrons})$ below 1 GeV?

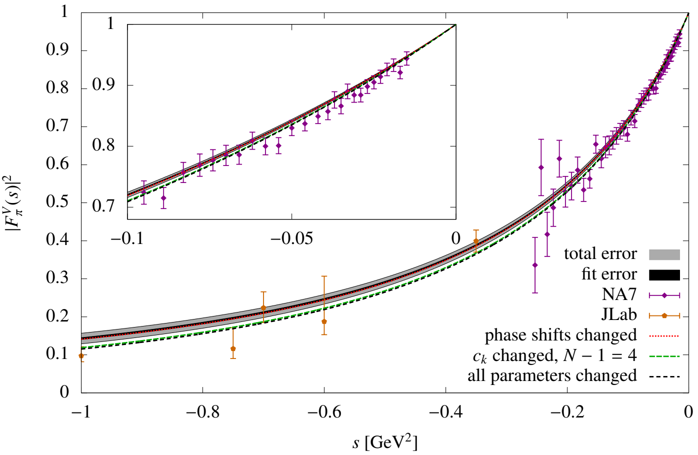


GC, Hoferichter, Stoffer (21)

# BMW vs individual $\pi^+\pi^-$ experiments

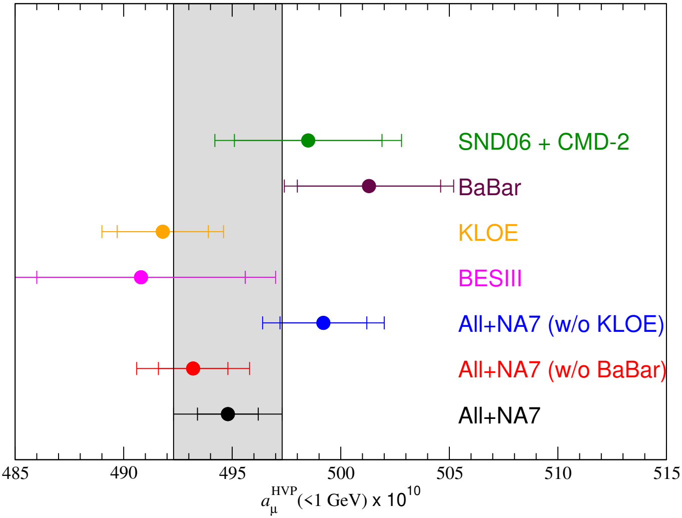

# BMW vs individual $\pi^+\pi^-$ experiments

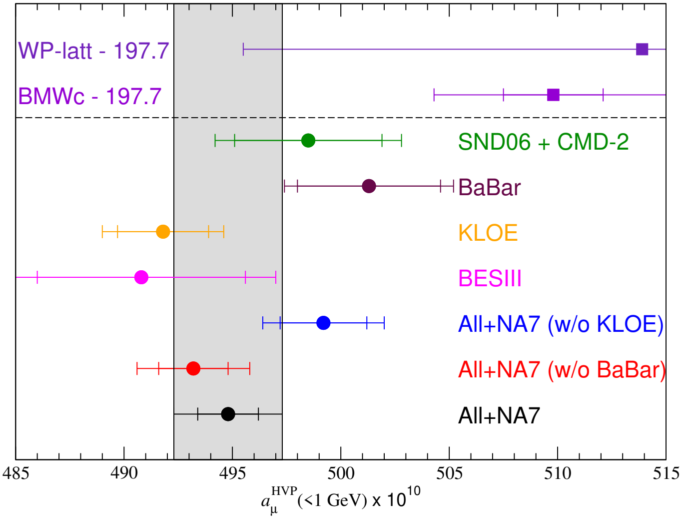

# BMW vs individual $\pi^+\pi^-$ experiments

**Article**

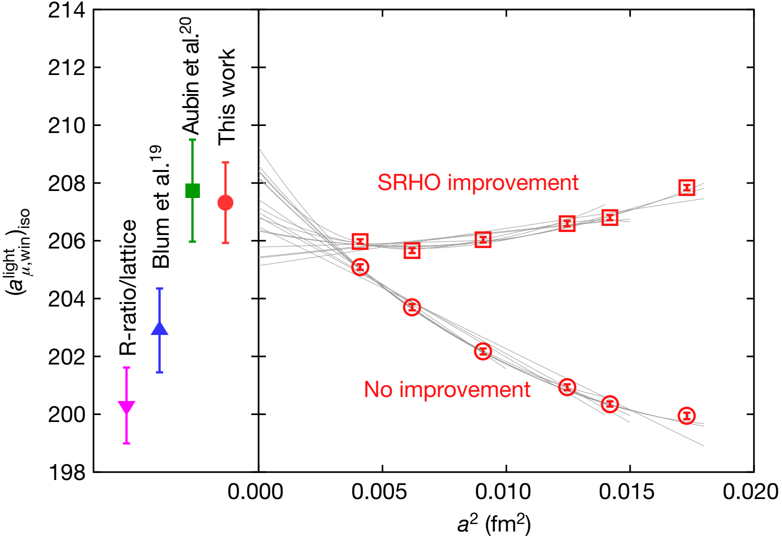

# BMW vs individual $\pi^+\pi^-$ experiments

## Weight functions for the window quantities

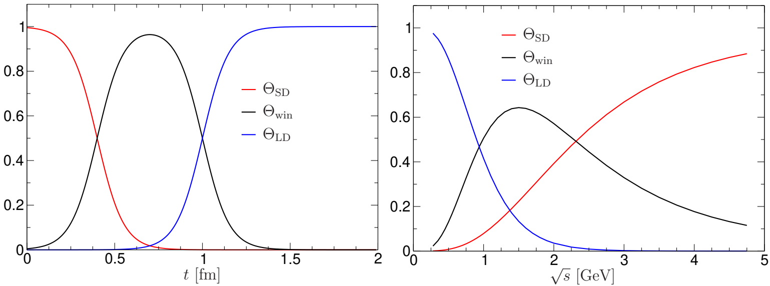

# BMW vs individual $\pi^+\pi^-$ experiments

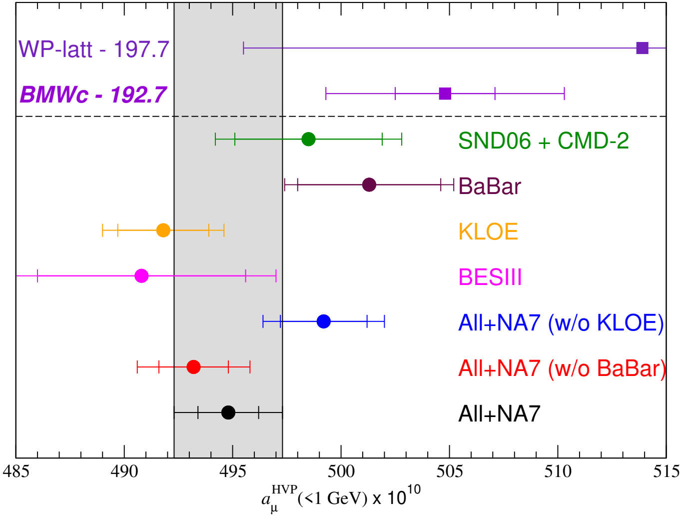


$a_\mu^{\rm win}$ suggests that $\sim 5\times 10^{-10}$ must come from above 1 GeV

GC, Hoferichter, Stoffer

# Outline

# Calculating the HLbL contribution

The HLbL contribution is a very complex quantity

- 4-point function of em currents in QCD

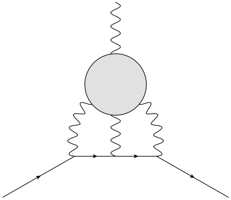

- early on, it has been calculated with models

  Hayakawa-Kinoshita-Sanda/Bijnens-Pallante-Prades (96), Knecht, Nyffeler (02), Melnikov, Vainshtein (04)

- a data-driven approach, like for HVP, has only recently been developed and used

  GC, Hoferichter, Procura, Stoffer=CHPS (14,15,17), Hoferichter, Hoid, Kubis, Leupold, Schneider (18)

- lattice QCD is becoming competitive

  RBC/UKQCD (20), Mainz (21)

# Different model-based evaluations of HLbL

Jegerlehner-Nyffeler 2009

| Contribution | BPaP(96) | HKS(96) | KnN(02) | MV(04) | BP(07) | PdRV(09) | N/JN(09) |
|---|---|---|---|---|---|---|---|
| $\pi^0, \eta, \eta'$ | 85±13 | 82.7±6.4 | 83±12 | 114±10 | – | 114±13 | 99±16 |
| $\pi$, $K$ loops | −19±13 | −4.5±8.1 | – | – | – | −19±19 | −19±13 |
| " " + subl. in $N_c$ | – | – | – | 0±10 | – | – | – |
| axial vectors | 2.5±1.0 | 1.7±1.7 | – | 22± 5 | – | 15±10 | 22± 5 |
| scalars | −6.8±2.0 | – | – | – | – | −7± 7 | −7± 2 |
| quark loops | 21± 3 | 9.7±11.1 | – | – | – | 2.3 | 21± 3 |
| total | 83±32 | 89.6±15.4 | 80±40 | 136±25 | 110±40 | 105±26 | 116±39 |

Legenda: B=Bijnens Pa=Pallante P=Prades H=Hayakawa K=Kinoshita S=Sanda Kn=Knecht N=Nyffeler M=Melnikhov V=Vainshtein dR=de Rafael J=Jegerlehner

- large uncertainties (and differences among calculations) in individual contributions
- pseudoscalar pole contributions most important
- second most important: pion loop, *i.e.* two-pion cuts (*Ks are subdominant*)
- heavier single-particle poles decreasingly important

# Advantages of the dispersive approach

- model independent
- unambiguous definition of the various contributions
- makes a data-driven evaluation possible
  (in principle)
- if data not available: use theoretical calculations of subamplitudes, short-distance constraints etc.

# Advantages of the dispersive approach

- model independent
- unambiguous definition of the various contributions
- makes a data-driven evaluation possible (in principle)
- if data not available: use theoretical calculations of subamplitudes, short-distance constraints etc.
- First attempts: GC, Hoferichter, Procura, Stoffer (14)
  Pauk, Vanderhaeghen (14)
- similar philosophy, with a different implementation: Schwinger sum rule Hagelstein, Pascalutsa (17)
- why hasn't this been adopted before?

# Hadronic vacuum polarization

$$\Pi_{\mu\nu}(q) = i\int d^4x e^{iqx}\langle 0|Tj_\mu(x)j_\nu(0)|0\rangle = \left(q_\mu q_\nu - g_{\mu\nu}q^2\right)\Pi(q^2)$$

where $j^\mu(x) = \sum_i Q_i\bar{q}_i(x)\gamma^\mu q_i(x)$, $i = u, d, s$ is the em current

- Lorentz invariance: 2 structures
- gauge invariance: reduction to 1 structure
- Lorentz-tensor defined in such a way that the function $\Pi(q^2)$ does not have kinematic singularities or zeros
- $\bar{\Pi}(q^2) := \Pi(q^2) - \Pi(0)$ satisfies

$$\bar{\Pi}(q^2) = \frac{q^2}{\pi}\int_{4M_\pi^2}^{\infty} dt \frac{\mathrm{Im}\bar{\Pi}(t)}{t(t-q^2)}$$

# Hadronic vacuum polarization

$$\Pi_{\mu\nu}(q) = i\int d^4x e^{iqx}\langle 0|T j_\mu(x) j_\nu(0)|0\rangle = \left(q_\mu q_\nu - g_{\mu\nu}q^2\right)\Pi(q^2)$$

where $j^\mu(x) = \sum_i Q_i \bar{q}_i(x)\gamma^\mu q_i(x)$, $i = u, d, s$ is the em current

- Lorentz invariance: 2 structures
- gauge invariance: reduction to 1 structure
- Lorentz-tensor defined in such a way that the function $\Pi(q^2)$ does not have kinematic singularities or zeros
- $\bar{\Pi}(q^2) := \Pi(q^2) - \Pi(0)$ satisfies

$$\bar{\Pi}(q^2) = \frac{q^2}{\pi}\int_{4M_\pi^2}^\infty dt \frac{\mathrm{Im}\bar{\Pi}(t)}{t(t-q^2)}$$

Easy!

# The HLbL tensor

HLbL tensor:

$$\Pi^{\mu\nu\lambda\sigma} = i^3 \int dx \int dy \int dz\, e^{-i(x\cdot q_1 + y\cdot q_2 + z\cdot q_3)} \langle 0 | T\{ j^\mu(x) j^\nu(y) j^\lambda(z) j^\sigma(0) \} | 0 \rangle$$

$$q_4 = k = q_1 + q_2 + q_3 \qquad k^2 = 0$$

General Lorentz-invariant decomposition:

$$\Pi^{\mu\nu\lambda\sigma} = g^{\mu\nu} g^{\lambda\sigma} \Pi^1 + g^{\mu\lambda} g^{\nu\sigma} \Pi^2 + g^{\mu\sigma} g^{\nu\lambda} \Pi^3 + \sum_{i,j,k,l} q_i^\mu q_j^\nu q_k^\lambda q_l^\sigma \Pi^4_{ijkl} + \dots$$

consists of 138 scalar functions $\{\Pi^1, \Pi^2, \dots\}$, but in $d = 4$ only 136 are linearly independent Eichmann *et al.* (14)

Constraints due to gauge invariance? (see also Eichmann, Fischer, Heupel (2015))

$\Rightarrow$ Apply the Bardeen-Tung (68) method+Tarrach (75) addition

# Gauge-invariant hadronic light-by-light tensor

Applying the Bardeen-Tung-Tarrach method to $\Pi^{\mu\nu\lambda\sigma}$ one ends up with: GC, Hoferichter, Procura, Stoffer ≡ CHPS (2015)

- 43 basis tensors (BT) — in $d=4$: 41=no. of helicity amplitudes
- 11 additional ones (T) — to guarantee basis completeness everywhere
- of these 54 only 7 are distinct structures
- all remaining 47 can be obtained by crossing transformations of these 7: manifest crossing symmetry
- the dynamical calculation needed to fully determine the HLbL tensor concerns these 7 scalar amplitudes

$$\Pi^{\mu\nu\lambda\sigma} = \sum_{i=1}^{54} T_i^{\mu\nu\lambda\sigma} \Pi_i$$

# Setting up the dispersive calculation

For HVP the unitarity relation is simple and looks the same for all possible intermediate states

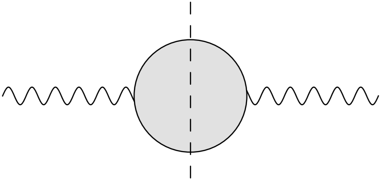

$$\mathrm{Im}\Pi(q^2) \propto \sigma(e^+e^- \to \mathrm{hadrons})$$

# Setting up the dispersive calculation

For HVP the unitarity relation is simple and looks the same for all possible intermediate states

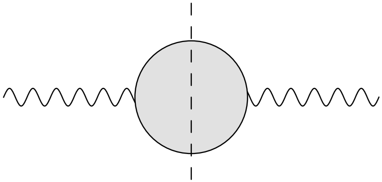

$$\mathrm{Im}\Pi(q^2) \propto \sigma(e^+e^- \to \text{hadrons})$$

For HLbL things are more complicated

# Setting up the dispersive calculation

We split the HLbL tensor as follows:

$$\Pi_{\mu\nu\lambda\sigma} = \Pi^{\pi^0\text{-pole}}_{\mu\nu\lambda\sigma} + \Pi^{\pi\text{-box}}_{\mu\nu\lambda\sigma} + \bar{\Pi}_{\mu\nu\lambda\sigma} + \cdots$$

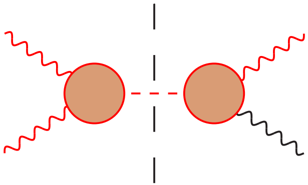

Pion pole: imaginary parts = $\delta$-functions
Projection on the BTT basis: easy ✓
Our master formula=explicit expressions in the literature ✓
Input: pion transition form factor — Hoferichter et al. (18)
First results of direct lattice calculations — Gerardin, Meyer, Nyffeler (16,19)

# Setting up the dispersive calculation

We split the HLbL tensor as follows:

$$\Pi_{\mu\nu\lambda\sigma} = \Pi^{\pi^0\text{-pole}}_{\mu\nu\lambda\sigma} + \Pi^{\pi\text{-box}}_{\mu\nu\lambda\sigma} + \bar{\Pi}_{\mu\nu\lambda\sigma} + \cdots$$

$\pi$-box with the BTT set:

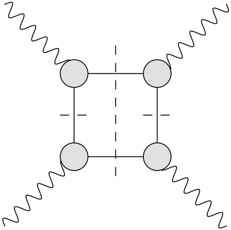

- we have constructed a Mandelstam representation for the contribution of the 2-pion cut with LHC due to a pion pole
- we have explicitly checked that this is identical to sQED multiplied by $F_\pi^V(s)$ (FsQED)

# Setting up the dispersive calculation

We split the HLbL tensor as follows:

$$\Pi_{\mu\nu\lambda\sigma} = \Pi^{\pi^0\text{-pole}}_{\mu\nu\lambda\sigma} + \Pi^{\pi\text{-box}}_{\mu\nu\lambda\sigma} + \bar{\Pi}_{\mu\nu\lambda\sigma} + \cdots$$

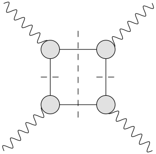

$$\equiv F_\pi^V(q_1^2)F_\pi^V(q_2^2)F_\pi^V(q_3^2)$$

$\times$

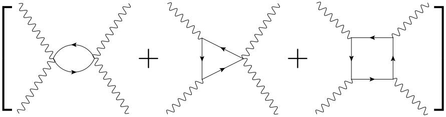

# Setting up the dispersive calculation

We split the HLbL tensor as follows:

$$\Pi_{\mu\nu\lambda\sigma} = \Pi^{\pi^0\text{-pole}}_{\mu\nu\lambda\sigma} + \Pi^{\pi\text{-box}}_{\mu\nu\lambda\sigma} + \bar{\Pi}_{\mu\nu\lambda\sigma} + \cdots$$

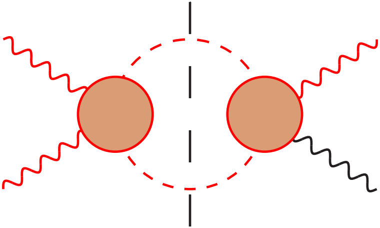

The "rest" with $2\pi$ intermediate states has cuts only in one channel and will be calculated dispersively after partial-wave expansion

# Setting up the dispersive calculation

We split the HLbL tensor as follows:

$$\Pi_{\mu\nu\lambda\sigma} = \Pi^{\pi^0\text{-pole}}_{\mu\nu\lambda\sigma} + \Pi^{\pi\text{-box}}_{\mu\nu\lambda\sigma} + \bar{\Pi}_{\mu\nu\lambda\sigma} + \cdots$$

Contributions of cuts with anything else other than one and two pions in intermediate states are neglected in first approximation

of course, the $\eta$, $\eta'$ and other pseudoscalars pole contribution, or the kaon-box/rescattering contribution can be calculated within the same formalism

# Pion-pole contribution

- Expression of this contribution in terms of the pion transition form factor already known Knecht-Nyffeler (01)
- Both transition form factors (TFF) are included:

$$\bar{\Pi}_1 = \frac{F_{\pi^0\gamma^*\gamma^*}(q_1^2, q_2^2) F_{\pi^0\gamma^*\gamma^*}(q_3^2, 0)}{q_3^2 - M_{\pi^0}^2}$$

- data on singly-virtual TFF available CELLO, CLEO, BaBar, Belle, BESIII
- several calculations of the transition form factors in the literature Masjuan & Sanchez-Puertas (17), Eichmann et al. (17), Guevara et al. (18)
- dispersive approach works here too Hoferichter et al. (18)
- lattice calculations can have a significant impact Gèrardin, Meyer, Nyffeler (16,19)

# Pion-pole contribution

Latest complete analyses:

- Dispersive calculation of the pion TFF — Hoferichter et al. (18)

$$a_\mu^{\pi^0} = 63.0^{+2.7}_{-2.1} \times 10^{-11}$$

- Padé-Canterbury approximants — Masjuan & Sanchez-Puertas (17)

$$a_\mu^{\pi^0} = 63.6(2.7) \times 10^{-11}$$

- Lattice — Gérardin, Meyer, Nyffeler (19)

$$a_\mu^{\pi^0} = 62.3(2.3) \times 10^{-11}$$

# Pion-box contribution

$$\Pi_{\mu\nu\lambda\sigma} = \Pi^{\pi^0\text{-pole}}_{\mu\nu\lambda\sigma} + \Pi^{\text{FsQED}}_{\mu\nu\lambda\sigma} + \bar{\Pi}_{\mu\nu\lambda\sigma} + \cdots$$

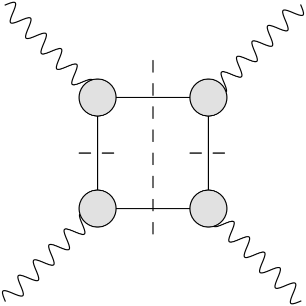

# Pion-box contribution

The only ingredient needed for the pion-box contribution is the vector form factor

$$\hat{\Pi}_i^{\pi\text{-box}} = F_\pi^V(q_1^2)F_\pi^V(q_2^2)F_\pi^V(q_3^2)\frac{1}{16\pi^2}\int_0^1 dx \int_0^{1-x} dy\, I_i(x,y),$$

where

$$I_1(x,y) = \frac{8xy(1-2x)(1-2y)}{\Delta_{123}\Delta_{23}},$$

and analogous expressions for $I_{4,7,17,39,54}$ and

$$\Delta_{123} = M_\pi^2 - xyq_1^2 - x(1-x-y)q_2^2 - y(1-x-y)q_3^2,$$
$$\Delta_{23} = M_\pi^2 - x(1-x)q_2^2 - y(1-y)q_3^2$$

# Pion-box contribution

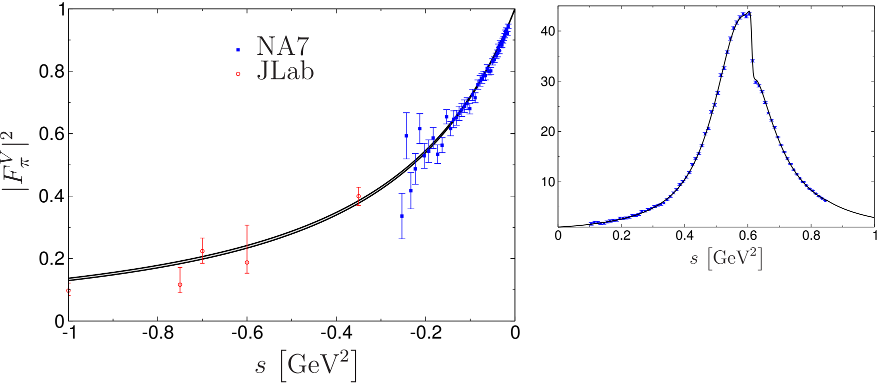


Uncertainties are negligibly small:

$$a_\mu^{\text{FsQED}} = -15.9(2) \cdot 10^{-11}$$

# Pion-box contribution

| Contribution | BPaP(96) | HKS(96) | KnN(02) | MV(04) | BP(07) | PdRV(09) | N/JN(09) |
|---|---|---|---|---|---|---|---|
| $\pi^0, \eta, \eta'$ | 85±13 | 82.7±6.4 | 83±12 | 114±10 | – | 114±13 | 99±16 |
| $\pi$, $K$ loops | −19±13 | −4.5±8.1 | – | – | – | −19±19 | −19±13 |
| " " + subl. in $N_c$ | – | – | – | 0±10 | – | – | – |
| axial vectors | 2.5±1.0 | 1.7±1.7 | – | 22± 5 | – | 15±10 | 22± 5 |
| scalars | −6.8±2.0 | – | – | – | – | −7± 7 | −7± 2 |
| quark loops | 21± 3 | 9.7±11.1 | – | – | – | 2.3 | 21± 3 |
| total | 83±32 | 89.6±15.4 | 80±40 | 136±25 | 110±40 | 105±26 | 116±39 |

Uncertainties are negligibly small:

$$a_\mu^{\text{FsQED}} = -15.9(2) \cdot 10^{-11}$$

# First evaluation of $S$- wave $2\pi$-rescattering

Omnès solution for $\gamma^*\gamma^* \to \pi\pi$ provides the following:

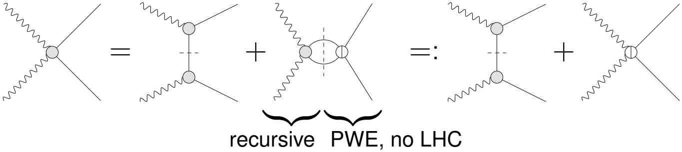


Based on:

- taking the pion pole as the only left-hand singularity
- $\Rightarrow$ pion vector FF to describe the off-shell behaviour
- $\pi\pi$ phases obtained with the inverse amplitude method

  [realistic only below 1 Gev: accounts for the $f_0(500)$ + unique and well defined extrapolation to $\infty$]
- numerical solution of the $\gamma^*\gamma^* \to \pi\pi$ dispersion relation

# First evaluation of $S$- wave $2\pi$-rescattering

Omnès solution for $\gamma^*\gamma^* \to \pi\pi$ provides the following:

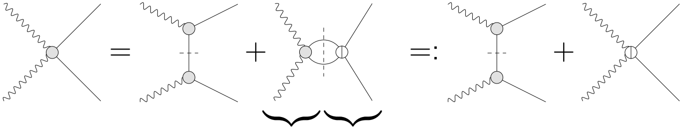


Based on:

- taking the pion pole as the only left-hand singularity
- $\Rightarrow$ pion vector FF to describe the off-shell behaviour
- $\pi\pi$ phases obtained with the inverse amplitude method
  [realistic only below 1 Gev: accounts for the $f_0(500)$ + unique and well defined extrapolation to $\infty$]
- numerical solution of the $\gamma^*\gamma^* \to \pi\pi$ dispersion relation

$S$-wave contributions : $a_{\mu,J=0}^{\pi\pi,\pi\text{-pole LHC}} = -8(1) \times 10^{-11}$

# Two-pion contribution to $(g-2)_\mu$ from HLbL

Two-pion contributions to HLbL:

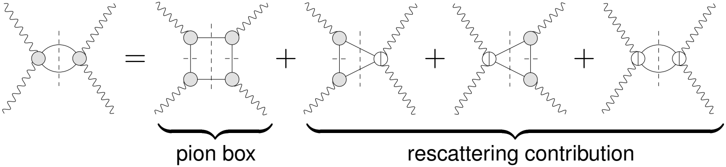


$$a_\mu^{\pi-\text{box}} + a_{\mu,J=0}^{\pi\pi,\pi\text{-pole LHC}} = -24(1)\cdot 10^{-11}$$

# Improvements obtained with the dispersive approach

| Contribution | PdRV(09) *Glasgow consensus* | N/JN(09) | J(17) | WP(20) |
|---|---|---|---|---|
| $\pi^0, \eta, \eta'$-poles | 114(13) | 99(16) | 95.45(12.40) | 93.8(4.0) |
| $\pi$, $K$-loops/boxes | −19(19) | −19(13) | −20(5) | −16.4(2) |
| $S$-wave $\pi\pi$ rescattering | −7(7) | −7(2) | −5.98(1.20) | −8(1) |
| subtotal | 88(24) | 73(21) | 69.5(13.4) | 69.4(4.1) |
| scalars | – | – | – | } − 1(3) |
| tensors | – | – | 1.1(1) | } |
| axial vectors | 15(10) | 22(5) | 7.55(2.71) | 6(6) |
| $u, d, s$-loops / short-distance | – | 21(3) | 20(4) | 15(10) |
| $c$-loop | 2.3 | – | 2.3(2) | 3(1) |
| total | 105(26) | 116(39) | 100.4(28.2) | 92(19) |

- significant reduction of uncertainties in the first three rows

  CHPS (17), Masjuan, Sánchez-Puertas (17) Hoferichter, Hoid et al. (18), Gerardin, Meyer, Nyffeler (19)

- 1 – 2 GeV resonances affected by basis ambiguity
- asymptotic region recently addressed, but still work in progress

  Melnikov, Vainshtein (04), Nyffeler (09), WP20, Bijnens et al. (20,21), GC, Hagelstein et al (19,21)

# Situation for HLbL

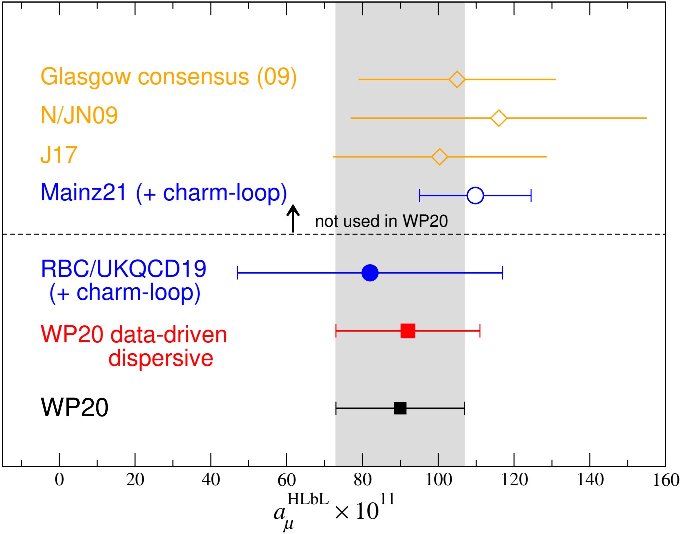

# Longitudinal SDCs: a few definitions

The longitudinal SDC only concerns one function: $\Pi_1$

Split $\pi^0$-pole from the rest in general kinematics ($q_4^2 = 0,\ q_4^\mu \neq 0$):

$$\Pi_1(s,t,u) = \frac{F_{\pi\gamma^*\gamma^*}(q_1^2,q_2^2)F_{\pi\gamma\gamma^*}(q_3^2)}{s-M_\pi^2} + G(s,t,u)$$

For $g-2$ kinematics ($q_4^\mu \to 0, \Rightarrow\ s = q_3^2,\ t = q_2^2,\ u = q_1^2$):

$$\begin{aligned}\bar\Pi_1(q_3^2,q_2^2,q_1^2) &= \frac{F_{\pi\gamma^*\gamma^*}(q_1^2,q_2^2)F_{\pi\gamma\gamma^*}(q_3^2)}{q_3^2-M_\pi^2} + G(q_3^2,q_2^2,q_1^2)\\ &= \frac{F_{\pi\gamma^*\gamma^*}(q_1^2,q_2^2)}{q_3^2-M_\pi^2}\left[F_{\pi\gamma\gamma^*}(M_\pi^2) + \bar F_{\pi\gamma\gamma^*}(q_3^2)\right] + G(q_3^2,q_2^2,q_1^2)\end{aligned}$$

with $\bar F_{\pi\gamma\gamma^*}(q_3^2) \equiv F_{\pi\gamma\gamma^*}(q_3^2) - F_{\pi\gamma\gamma^*}(M_\pi^2)$

# Longitudinal SDCs: a few definitions

The longitudinal SDC only concerns one function: $\Pi_1$

Split $\pi^0$-pole from the rest in general kinematics ($q_4^2 = 0,\ q_4^\mu \neq 0$):

$$\Pi_1(s,t,u) = \frac{F_{\pi\gamma^*\gamma^*}(q_1^2,q_2^2)F_{\pi\gamma\gamma^*}(q_3^2)}{s-M_\pi^2} + G(s,t,u)$$

For $g-2$ kinematics ($q_4^\mu \to 0, \Rightarrow\ s = q_3^2,\ t = q_2^2,\ u = q_1^2$):

$$\begin{aligned}\bar{\Pi}_1(q_3^2,q_2^2,q_1^2) &= \frac{F_{\pi\gamma^*\gamma^*}(q_1^2,q_2^2)F_{\pi\gamma\gamma^*}(q_3^2)}{q_3^2-M_\pi^2} + G(q_3^2,q_2^2,q_1^2)\\ &= \frac{F_{\pi\gamma^*\gamma^*}(q_1^2,q_2^2)}{q_3^2-M_\pi^2}\left[F_{\pi\gamma\gamma^*}(M_\pi^2) + \bar{F}_{\pi\gamma\gamma^*}(q_3^2)\right] + G(q_3^2,q_2^2,q_1^2)\end{aligned}$$

with $\bar{F}_{\pi\gamma\gamma^*}(q_3^2) \equiv F_{\pi\gamma\gamma^*}(q_3^2) - F_{\pi\gamma\gamma^*}(M_\pi^2)$

# The longitudinal SDCs

Two different kinematic configurations for large $q_i^2$:

1. All momenta large — Melnikov-Vainshtein (04), Bijnens et al (19)

$$\bar{\Pi}_1(q^2,q^2,q^2) \overset{q^2\to\infty}{=} -\frac{4}{9\pi^2 q^4} + \mathcal{O}(q^{-6})$$

2. $q^2 \equiv q_1^2 \sim q_2^2 \gg q_3^2,\ q^2 \gg \Lambda^2_{\mathrm{QCD}}$: — Melnikov-Vainshtein (04)

$$\bar{\Pi}_1(q_3^2,q^2,q^2) \overset{q^2\to\infty}{=} -\frac{1}{9\pi^2 q^2} w_L(q_3^2) + \mathcal{O}(q^{-4})$$

with $w_L(q_3^2)$ the longitudinal amplitude in $\langle VVA\rangle$, *the anomaly*

# The longitudinal SDCs

Two different kinematic configurations for large $q_i^2$:

1. All momenta large — Melnikov-Vainshtein (04), Bijnens et al (19)

$$\bar{\Pi}_1(q^2,q^2,q^2) \stackrel{q^2\to\infty}{=} -\frac{4}{9\pi^2 q^4} + \mathcal{O}(q^{-6})$$

2. $q^2 \equiv q_1^2 \sim q_2^2 \gg q_3^2,\ q^2 \gg \Lambda^2_{\rm QCD}$: — Melnikov-Vainshtein (04)

$$\bar{\Pi}_1(q_3^2,q^2,q^2) \stackrel{q^2\to\infty}{=} -\frac{1}{9\pi^2 q^2}\frac{6}{q_3^2} + \mathcal{O}(q^{-4})$$

In the chiral (and large-$N_c$) limit $w_L(q_3^2)$ is known exactly

$$w_L(q_3^2) = \frac{6}{q_3^2} \ \Rightarrow \ G(q_3^2,q^2,q^2)\Big|_{m_q=0} \stackrel{q\to\infty}{=} \frac{2F_\pi}{3q^2}\frac{\bar{F}_{\pi\gamma\gamma^*}(q_3^2)}{q_3^2}\Bigg|_{m_q=0} + \mathcal{O}(q^{-4})$$

No individual dispersive contribution satisfies these constraints

# The longitudinal SDCs

Two different kinematic configurations for large $q_i^2$:

1. All momenta large — Melnikov-Vainshtein (04), Bijnens et al (19)

$$\bar{\Pi}_1(q^2,q^2,q^2) \overset{q^2\to\infty}{=} -\frac{4}{9\pi^2 q^4} + \mathcal{O}(q^{-6})$$

2. $q^2 \equiv q_1^2 \sim q_2^2 \gg q_3^2,\ q^2 \gg \Lambda^2_{\mathrm{QCD}}$: — Melnikov-Vainshtein (04)

$$\bar{\Pi}_1(q_3^2,q^2,q^2) \overset{q^2\to\infty}{=} -\frac{1}{9\pi^2 q^2}\frac{6}{q_3^2} + \mathcal{O}(q^{-4})$$

In the chiral (and large-$N_c$) limit $w_L(q_3^2)$ is known exactly

$$w_L(q_3^2) = \frac{6}{q_3^2} \ \Rightarrow\ G(q_3^2,q^2,q^2)\Big|_{m_q=0} \overset{q\to\infty}{=} \frac{2F_\pi}{3q^2}\frac{\bar{F}_{\pi\gamma\gamma^*}(q_3^2)}{q_3^2}\Big|_{m_q=0} + \mathcal{O}(q^{-4})$$

The $\pi$-pole for $g-2$ kinematics does — Melnikov-Vainshtein (04)

# Recent activity on SDCs (mainly post WP)

- calculation of (non-)perturbative corrections to the OPE

  Bijnens, Hermansson-Truedsson, Laub, Rodríguez-Sánchez (20,21)

- tower of excited pseudoscalars (Regge model)

  GC, Hagelstein, Hoferichter, Laub, Stoffer (19)

- tower of axial-vectors (holographic QCD model)

  Leutgeb, Rebhan (19), Cappiello, Catà, D'Ambrosio, Greynat, Iyer (20)

- solution based on interpolants

  Lüdtke, Procura (20)

- general considerations, comparison of model solutions

  Knecht (20), Masjuan, Roig, Sánchez-Puertas (20), GC, Hagelstein, Hoferichter, Laub, Stoffer (21)

# Recent activity on SDCs (mainly post WP)

- calculation of (non-)perturbative corrections to the OPE

  Bijnens, Hermansson-Truedsson, Laub, Rodríguez-Sánchez (20,21)

- tower of excited pseudoscalars (Regge model)

  GC, Hagelstein, Hoferichter, Laub, Stoffer (19)

- tower of axial-vectors (holographic QCD model)

  Leutgeb, Rebhan (19), Cappiello, Catà, D'Ambrosio, Greynat, Iyer (20)

- solution based on interpolants

  Lüdtke, Procura (20)

- general considerations, comparison of model solutions

  Knecht (20), Masjuan, Roig, Sánchez-Puertas (20), GC, Hagelstein, Hoferichter, Laub, Stoffer (21)

# Melnikov-Vainshtein and holographic QCD

- Melnikov-Vainshtein model: Melnikov-Vainshtein (04)

$$w_L^{\rm MV}(q_3^2) = \frac{6}{q_3^2 - M_\pi^2} + \mathcal{O}(M_\pi^2)$$

$$G^{\rm MV}(q_i^2) = -\frac{F_{\pi\gamma^*\gamma^*}(q_1^2, q_2^2)\bar{F}_{\pi\gamma\gamma^*}(q_3^2)}{q_3^2} + \mathcal{O}(M_\pi^2)$$

- hQCD (HW2) model: Leutgeb, Rebhan (19), Cappiello et al. (20)

$$w_L^{\rm HW2}(q_3^2) = \frac{6}{q_3^2 - M_\pi^2}\left[1 + \frac{M_\pi^2 \bar{F}_{\pi\gamma\gamma^*}(q_3^2)}{q_3^2 F_{\pi\gamma\gamma}}\right]$$

$$G^{\rm HW2}(q_i^2) = -\frac{F_{\pi\gamma^*\gamma^*}(q_1^2, q_2^2)\bar{F}_{\pi\gamma\gamma^*}(q_3^2)}{q_3^2} - \frac{F_{\pi\gamma\gamma}^2}{q_3^2}\Delta G(q_i^2)$$

# Melnikov-Vainshtein and holographic QCD

- Melnikov-Vainshtein model: Melnikov-Vainshtein (04)

$$w_L^{\text{MV}}(q_3^2) = \frac{6}{q_3^2 - M_\pi^2} + \mathcal{O}(M_\pi^2)$$

$$G^{\text{MV}}(q_i^2) = -\frac{F_{\pi\gamma^*\gamma^*}(q_1^2, q_2^2)\bar{F}_{\pi\gamma\gamma^*}(q_3^2)}{q_3^2} + \mathcal{O}(M_\pi^2)$$

- hQCD (HW2) model: Leutgeb, Rebhan (19), Cappiello et al. (20)

$$w_L^{\text{HW2}}(q_3^2) = \frac{6}{q_3^2 - M_\pi^2}\left[1 + \frac{M_\pi^2 \bar{F}_{\pi\gamma\gamma^*}(q_3^2)}{q_3^2 F_{\pi\gamma\gamma}}\right]$$

$$G^{\text{HW2}}(q_i^2) = -\frac{F_{\pi\gamma^*\gamma^*}(q_1^2, q_2^2)\bar{F}_{\pi\gamma\gamma^*}(q_3^2)}{q_3^2} - \frac{F_{\pi\gamma\gamma}^2}{q_3^2}\Delta G(q_i^2)$$

$$\equiv \quad MV(q_i^2) \quad + \quad NF(q_i^2)$$

# Numerical comparison for $w_L$

GC, Hagelstein, Hoferichter, Laub, Stoffer (21)

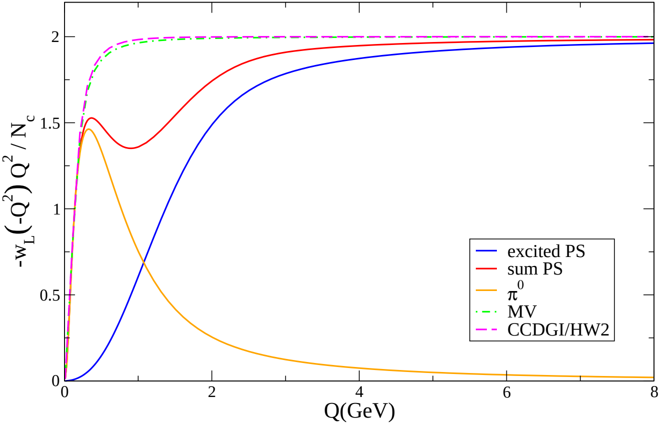

# Numerical comparison for $G$

GC, Hagelstein, Hoferichter, Laub, Stoffer (21)

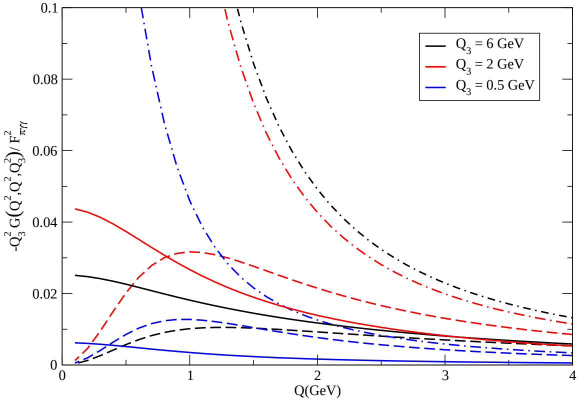


Legenda: dashed=CCDGI/HW2, dotdashed=MV, solid=PS Regge

# Numerical comparison for $G$

GC, Hagelstein, Hoferichter, Laub, Stoffer (21)

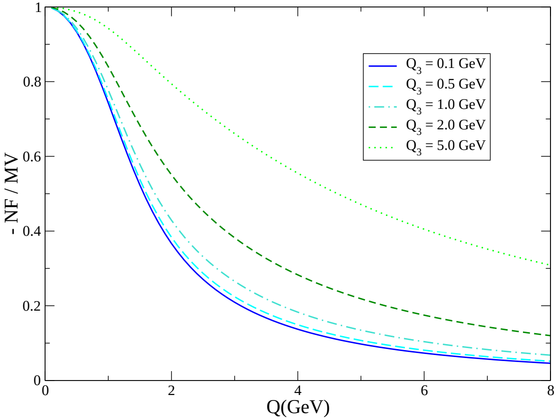

# Numerical comparison for $a_\mu^{\text{HLbL}}$

GC, Hagelstein, Hoferichter, Laub, Stoffer (21)

| | MV model | CCDGI set 1 | CCDGI set 2 | LR HW2 | LR HW2$_{\text{UV-fit}}$ | PS Regge model |
|---|---|---|---|---|---|---|
| | | | $\Delta a_\mu^{\pi/a_1} \times 10^{11}$ | | | |
| $Q_i^2 > Q_{\text{match}}^2 \quad \forall i$ | 1.4 | 0.5 | 0.8 | 0.6 | 0.8 | 0.7 |
| $Q_{1,2}^2 > Q_{\text{match}}^2 > Q_3^2$ | 0.1 | 0.0 | 0.1 | 0.0 | 0.1 | 0.1 |
| $Q_{i,3}^2 > Q_{\text{match}}^2 > Q_j^2 \quad i \neq j \neq 3$ | 2.0 | 1.0 | 1.2 | 1.0 | 1.2 | 0.7 |
| $Q_i^2 > Q_{\text{match}}^2 > Q_{j,k} \quad i \neq j \neq k$ | 0.8 | 0.3 | 0.4 | 0.3 | 0.3 | 0.2 |
| $Q_{\text{match}}^2 > Q_i^2 \quad \forall i$ | 11.8 | 2.2 | 1.7 | 2.3 | 1.8 | 1.0 |
| Total | 16.2 | 4.0 | 4.2 | 4.2 | 4.3 | 2.7 |
| | | | $\Delta a_\mu^{\eta/f_1+\eta'/f_1'} \times 10^{11}$ | | | |
| $Q_i^2 > Q_{\text{match}}^2 \quad \forall i$ | 3.4 | 1.3 | 1.7 | 1.7 | 2.5 | 3.1 |
| $Q_{1,2}^2 > Q_{\text{match}}^2 > Q_3^2$ | 0.3 | 0.1 | 0.2 | 0.1 | 0.2 | −0.1 |
| $Q_{i,3}^2 > Q_{\text{match}}^2 > Q_j^2 \quad i \neq j \neq 3$ | 3.7 | 2.5 | 2.8 | 3.0 | 3.7 | 2.8 |
| $Q_i^2 > Q_{\text{match}}^2 > Q_{j,k} \quad i \neq j \neq k$ | 1.7 | 0.8 | 0.9 | 0.9 | 0.9 | 0.9 |
| $Q_{\text{match}}^2 > Q_i^2 \quad \forall i$ | 12.9 | 5.6 | 5.1 | 6.8 | 5.5 | 3.1 |
| Total | 22.1 | 10.3 | 10.7 | 12.5 | 12.8 | 9.9 |
| Grand total $(\pi/a_1 + \eta/f_1 + \eta'/f_1')$ | 38.3 | 14.3 | 14.9 | 16.7 | 17.1 | 12.6 |

# Numerical comparison for $a_\mu^{\text{HLbL}}$

GC, Hagelstein, Hoferichter, Laub, Stoffer (21)

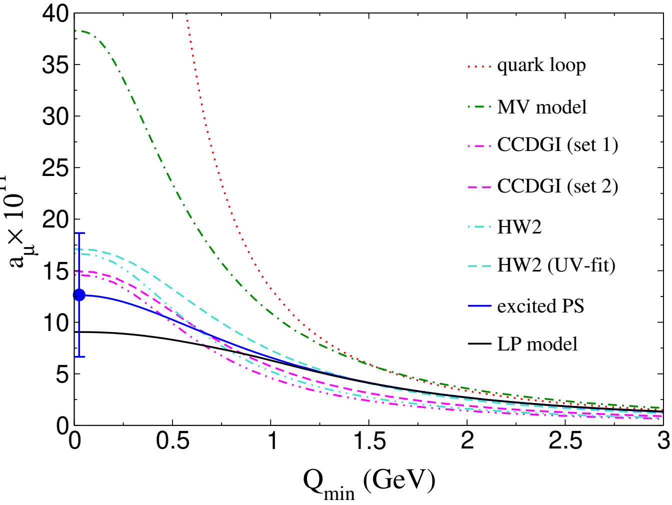

# Outline

# Conclusions

- The WP provides the current status of the SM evaluation of $(g-2)_\mu$: $4.2\sigma$ discrepancy with experiment (w/ FNAL)
- Evaluation of the HVP contribution based on the dispersive approach: 0.6% error $\Rightarrow$ dominates the theory uncertainty
- Recent lattice calculation [BMW(20)] has reached a similar precision but differs from the dispersive one (=from $e^+e^-$ data).
  If confirmed $\Rightarrow$ discrepancy with experiment $\searrow$ below $2\sigma$
- Evaluation of the HLbL contribution based on the dispersive approach: 20% accuracy. Two recent lattice calculations [RBC/UKQCD(20), Mainz(21)] agree with it

# Outlook

- The Fermilab experiment aims to reduce the BNL uncertainty by a factor four $\Rightarrow$ potential $7\sigma$ discrepancy
- Improvements on the SM theory/data side:
  - HVP data-driven:
    Other $e^+e^-$ experiments are available or forthcoming:
    SND, BaBar, Belle II, BESIII, CMD3 $\Rightarrow$ Error reduction
    MuonE will provide an alternative way to measure HVP
  - HVP lattice:
    More calculations w/ precision $\sim$ BMW are awaited
    Difference to data-driven evaluation must be understood
  - HLbL data-driven: goal of $\sim$ 10% uncertainty within reach
  - HLbL lattice: RBC/UKQCD $\Rightarrow$ similar precision as Mainz.
    Good agreement with data-driven evaluation.

# Future: Muon $g-2$/EDM experiment @ J-PARC

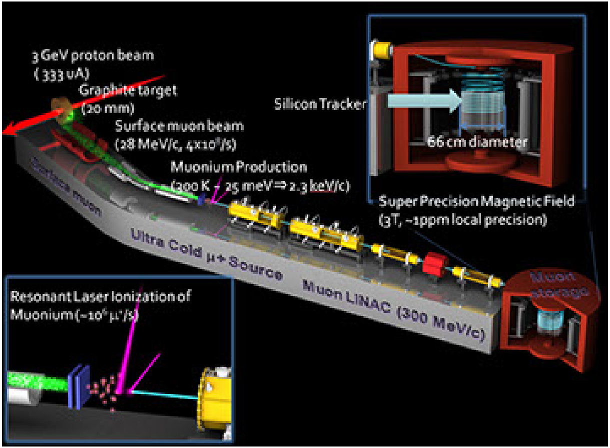


Credit: J-PARC